J. Plasma Physics (2001), vol. 66, parts 1 & 2, pp. 39–51. © 2001 Cambridge University Press 
DOI: 10.1017/S0022377801001258 Printed in the United Kingdom

# Two-dimensional self-focusing of a laser beam in an inhomogeneous laser-produced plasma

TARSEM SINGH GILL,[1] NARESHPAL SINGH SAINI[1] and SHYAM SUNDER KAUL[2]

[1]Department of Physics, Guru Nanak Dev University, Amritsar 143005, India
[2]Department of Physics, Sikh National College, Banga 144505, India

(Received 1 February 2000 and in revised form 15 February 2001)

**Abstract.** Self-focusing is one of the key issues in laser plasma physics applications. Problems involving a multidimensional beam within an inhomogeneous plasma are difficult to handle. This paper presents the investigation of two-dimensional self-focusing of a laser beam in a plasma whose density $n(r, z)$ is a function of radial as well as $z$ coordinates. The nonlinear mechanism responsible for modification of the background density and the dielectric function is of ponderomotive type. A variational technique is used here for deriving the equations for the beam width and the longitudinal phase. It is observed numerically that an initially diffracting beam is accompanied by oscillatory self-focusing of the beam with distance of propagation. The effect of inhomogeneity scale lengths is also observed. The increase in $L_r$ $(= L_{\|}/L_{\perp})$ results in oscillatory self-focusing and defocusing with distance of propagation. Furthermore, critical fields for self-trapping of a laser beam as a function of refraction, diffraction lengths and scale lengths of inhomogeneities are also evaluated. Lastly, whatever parameters are chosen, the phase is always negative.

## 1. Introduction

In a nonlinear medium, if a high-power electromagnetic beam increases the electric susceptibility and thus the refractive index with wave intensity, then in a region where the wave amplitude is slightly amplified, the refractive index is also enhanced. From the viewpoint of geometrical optics, the light rays bend towards this region, which further increases the refractive index and consequently bends the light rays even more. The beam thus creates a refractive-index profile across its cross-section corresponding to its own intensity profile, and focuses itself. The phenomenon was predicted by Askar'yan (1962), and is called self-focusing of radiation. It has been extensively studied in this context of laser-beam propagation since the early 1960s (Chio et al. 1964; Talanov 1965; Kelly 1965; Akhmanov et al. 1968; Perkins and Valeo 1974; Max 1976; Sodha et al. 1976; Lam and Lippman 1977; Anderson et al. 1979; Cohen et al. 1991; Malkin 1993; Berge 1997). Research into this process has acquired further importance with the availability of very high-power laser beam facilities such as the National Ignition Facility (Paisner et al. 1994) because of its relevance to inertial-confinement fusion plasmas. It is required that intense laser beams be propagated through long-scale underdense plasmas to achieve successful controlled nuclear fusion. However, such a situation is prone to vigorous growth of

https://doi.org/10.1017/S0022377801001258 Published online by Cambridge University Press

laser–plasma instabilities (Kruer 1988). Among the instabilities having deleterious effects, self-focusing and filamentation are the key ones to be understood and resolved (Kaw et al. 1973; Schmidt 1988; Berger et al. 1993). In the so-called hotspots of the laser beam, self-focusing or filamentation grows unstably through a feedback mechanism of increased electron thermal pressure and ponderomotive force. The latter two reinforce each other to expel the plasma, resulting in increased refractive index, which leads to further concentration of intensity in the regions of hotspots. The overall effect is distortion of the propagation characteristics of incident beam, poor efficiency of beam energy coupling to the target, and loss of symmetry of energy deposition leading to hydrodynamic instabilities of the target.

Theoretical investigations of self-focusing of laser beams in plasmas have been carried out by a number of researchers during the past three and half decades. They have used WKB and paraxial-ray approximations (Akhmanov et al. 1968; Sodha et al. 1976, 1981; Subbarao 1998; Sughiara and Nishimura 1995). As discussed by Wagner et al. (1968), the trial function is substituted into the evolution equation, where the nonlinear refractive index is Taylor-expanded in the transverse direction. The procedure was generalized to include the phase dynamics (Akhmanov et al. 1968). The alternative approach of moment theory (Lam and Lippman 1977; Vlasov et al. 1971; Zakharov 1972) is based on certain moments, and the evolution of transverse coordinates is considered. In spite of their mathematical simplicity, these theories give qualitatively good results.

A model frequently used to describe the self-focusing of laser beam in a Kerr medium with quadratic nonlinearity is

$$\left(i\frac{\partial}{\partial z} + \nabla_\perp^2 + |\mathbf{E}|^2\right)\mathbf{E} = 0 \tag{1}$$

Here $\mathbf{E}$ is the envelope of the electric field, $\nabla_\perp^2$ is the Laplacian in the transverse direction, and $z$ is the direction of propagation. The dynamics of self-focusing described by (1) is determined by the relative competition between spatial dispersion that spreads the beam in transverse direction and attracting nonlinearity that compresses the beam. When the nonlinearity overbalances the dispersion, beam collapse occurs and a singularity in $\mathbf{E}$ is formed. Problems of singularity formation and collapse have been discussed in detail elsewhere (Sulem and Sulem 1999).

Here, we consider the propagation dynamics of a beam undergoing self-focusing in an underdense plasma. Several parametric processes occur long before the critical surface is approached. However, an oscillating two-stream instability – a purely growing instability – occurs near the critical surface. Although there is interplay between some of these nonlinear processes for example coupled stimulated Raman scattering (SRS) and stimulated Brillouin scattering (SBS), self-focusing is supposed to influence these coupled processes (Amin et al. 1993). Our aim in this paper is to investigate the self-focusing process alone in an inhomogeneous plasma. We use here the model of Andreev et al. (1987). Earlier several investigators considered one-dimensional self-focusing (Akhmanov et al. 1968; Max 1976; Sodha et al. 1976). In such cases, plasmas are considered inhomogeneous in the transverse direction and homogeneous in the direction of propagation. Nonlinearity of types collisional, ponderomotive, or relativistic type (Max 1976; Sodha et al. 1976, 1981) causes redistribution of the carriers along the wavefront, modifying the background density, which results in self-induced inhomogeneity in the radial direction only. However, plasmas are inhomogeneous in nature, and to account for such plasmas, Andreev

https://doi.org/10.1017/S0022377801001258 Published online by Cambridge University Press

et al. (1987) considered a more realistic model. They did so to account for experimental results where filaments of dimensions 5–20 $\mu$m were observed during the interaction of a laser beam with a corona plasma. Such an inhomogeneous plasma leads to qualitatively new features in the formation of a transport channel and the self-focusing of the laser beam. The situation is also quite similar to the existence of a preformed plasma used in laser-guiding schemes where a nonuniform plasma channel is formed by a prepulse. Another case resembling this situation is the propagation of intense radio waves through an ionospheric plasma. Although this may be referred to as enhanced focusing, we refer to it as self-focusing, since transverse inhomogeneity combines with the effect of the ponderomotive term (the last term in (9)). Specifically, in laser–plasma interaction, plasmas that are nonuniform in the propagation direction up to the critical density are considered. Andreev et al. (1987), who investigated this problem, considered an inhomogeneous plasma by assuming inhomogeneity in two directions. This approach is relevant in the sense that plasmas of different scale lengths are produced, depending on the pulse duration. Since long-scale-length plasmas are required for inertial-confinement fusion, the relevant physics issues such as dependence of the propagation characteristics of the beam on different scale lengths must be investigated. Even though moment theory was used earlier to establish the condition for self-focusing, in later investigations, Andreev et al. (1987) used the paraxial-ray approximation to set up an equation for the beam-width parameter (cf. equation (2.1) of Andreev et al. 1987). Recently, Subbarao et al. (1998) have pointed out that the popular theory (Akhmanov et al. 1968; Max 1976; Sodha et al. 1974) based on a paraxial-ray approximation should be used only when low-power laser beams are considered. Preferably, moment theory or a variational approach or a corrected version of the paraxial-ray approximation (Subbarao et al. 1998) should be used for high-power laser beams. A variational approach that is approximately analytical, but fairly general in nature, is used here. This approach has also been used recently for self-focusing in a laser speckle (Tikhonchuk et al. 1997). Furthermore, it is reported to give a correct phase description (Karlsson et al. 1992). The limitation of the variational approach is that it is not suitable for the study of collapse and singularity formation, but we are not investigating such a problem here.

In this paper, a Gaussian laser beam as a trial function is considered. Section 2 deals with the basic formulation of the problem, where the Lagrangian for the problem is set up and the reduced variational problem is derived. Section 3 is devoted to discussions of the important results.

## 2. Basic formulation

We begin with the usual assumption that the field of the laser beam can be described by the scalar Helmholtz equation

$$\left(\frac{\partial^2}{\partial z^2} + \nabla_\perp^2\right)\mathbf{E} + k_0^2\epsilon(\mathbf{r}, |\mathbf{E}|^2)\mathbf{E} = 0, \tag{2}$$

where $k_0 = \omega_0/c$, with $\omega_0$ as the angular frequency and $c$ the velocity of light in vacuum. The dielectric function and other parameters in the case of ponderomotive nonlinearity are given as follows (Andreev et al. 1987):

$$\epsilon(\mathbf{r}, |\mathbf{E}|^2) = 1 - \frac{n_0(\mathbf{r})}{n_c} e^{-|\mathbf{E}|^2/E_p^2}, \tag{3}$$

https://doi.org/10.1017/S0022377801001258 Published online by Cambridge University Press

$$n_c = \frac{m\omega^2}{4\pi e^2}, \tag{4}$$

$$E_p^2 = 16\pi n_c k_B (T_e + T_i). \tag{5}$$

Here $n_c$ is the cut-off density, $k_B$ is Boltzmann's constant, and $T_e$ and $T_i$ are the electron and ion temperatures respectively. The field $E_p$ is typically the field of nonlinearity given by (5). We use the model of Andreev et al. (1987) with a two-dimensional background variation of the plasma density given as

$$n_0(\mathbf{r}) = n_1(z) + n_2(\mathbf{r}_\perp), \tag{6}$$

where $n_2 \ll n_1$.

Further, under the assumption of smooth longitudinal variation, it is possible to employ a parabolic approximation to solve (2) outside a small neighbourhood of the critical density surface $n_0(\mathbf{r}_c) = n_c$:

$$\mathbf{E}(z, \mathbf{r}_\perp) = \boldsymbol{\varepsilon}(z, \mathbf{r}_\perp) N_\parallel^{-1/2}(z) \exp\left[-ik_0 \int_0^z N_\parallel(z')\, dz'\right], \tag{7}$$

where

$$N_\parallel(z) = \left[1 - \frac{n_1(z)}{n_c}\right]^{1/2},$$

$$n_1(z) = \frac{n_c z}{L_\parallel}$$

for $0 < z < L_\parallel$. Here $L_\parallel$ is the longitudinal scale length and the longitudinal profile is

$$N_\parallel(z) = \left(1 - \frac{z}{L_\parallel}\right)^{1/2}, \tag{8}$$

With (7) substituted into (2) and using the WKB approximation, we get the nonlinear Schrödinger equation with exponential nonlinearity:

$$2ik_0 \frac{\partial \varepsilon}{\partial \xi} = \nabla_\perp^2 \varepsilon + k_0^2 \left[\frac{n_1}{n_c}(1 - e^{-I}) - \frac{n_2}{n_c} e^{-I}\right] \varepsilon, \tag{9}$$

where

$$\xi(z) = \int_0^z \frac{1}{N_\parallel(z')}\, dz' \tag{10}$$

$$n_2 = \frac{n_c r_\perp^2}{L_\perp^2},$$

and

$$I = \frac{|\varepsilon|^2}{[1 - n_1(z)/n_c]^{1/2} E_p^2}. \tag{11}$$

Here $L_\perp$ is the transverse scale length. Both longitudinal variation of density as well as transverse density profiles are introduced here. As mentioned earlier, addition of $n_2$ here leads to the existence of a preformed plasma channel. However, in the absence of $n_2$, the first term in the square brackets in (9) contributes to self-focusing and the problem reduces to earlier work of Andreev (1983) with longitudinal inhomogeneity only. This feature becomes more apparent in our calculations, where we have plotted the normalized beam width as a function of the dimensionless distance

https://doi.org/10.1017/S0022377801001258 Published online by Cambridge University Press

of propagation. Equation (9) is the same as that derived earlier (cf. equation (1.2) of Andreev et al. 1987).

Equation (9) although nonintegrable, conserves the following invariant:

$$Q = \int |\varepsilon|^2 r_\perp \, dr_\perp. \tag{12}$$

Equation (12) implies that the power is conserved and hence $|\varepsilon_0|^2 \pi a^2 = \text{const}$, and gives an explicit reference as to how the beam radius relates to the beam amplitude. It may be mentioned that the invariant (12) is a consequence of the symmetry relative to phase shift. Equation (9) also conserves the Hamiltonian

$$H = \int \left[ r \left| \frac{\partial \varepsilon}{\partial r} \right|^2 - F(I) \right] r_\perp \, dr_\perp \tag{13}$$

where

$$F(I) = \int_0^I G(I) \, dI$$

with

$$G(I) = \left[ \frac{n_1}{n_c}(1 - e^{-I}) - \frac{n_2}{n_c} e^{-I} \right]. \tag{14}$$

Conservation of the Hamiltonian results from the conservation of translational invariance in $\xi$. Similarly, invariance relative to spatial variation in $x$ and $y$ is related to conservation of momentum.

The conservation laws enunciated above do not hold if we consider (2) as such with fast variation included in the amplitude. It is only in the slowly varying envelope approximation (WKB approximation) that $\partial^2 E/\partial z^2$ is replaced by the first term in (2), leading to invariants of (9).

It must further be mentioned that $|\varepsilon|^2/E_p^2$ is dimensionless parameter, which determines the intensity of beam required for self-focusing. It can be shown that $|\varepsilon|^2/E_p^2$ is equivalent to $\frac{3}{4}\alpha(m/M)E_0^{-2}$, where $\alpha$ is a nonlinearity parameter. The importance of this parameter can be realized from a graph of $(r_0\omega_p/c)^2$ versus $\frac{3}{4}\alpha \frac{m}{M} E_0^2$ (Sodha et al. 1976). These two terms $(r_0\omega_p/c)^2$ and $|\varepsilon|^2/E_p^2$ together determine the threshold intensity for self-trapping. Since an exact solution of (9) is not available, one must use numerical or approximate analytical methods. The variational approach, although heuristic in nature, is used where the solution is assumed to maintain a prescribed approximate profile. Such methods simplify the problem, reducing it to a system of ordinary differential equations for the evolution of a few parameters. However, the method may not be able to capture the delicate balance associated with the critical collapse (Berge 1998), although it can be fairly satisfactorily used to study self-focusing in an underdense plasma. Moreover, the method is also not applicable in the vicinity of critical surface, since the assumption of smooth variation of $N_\|$ assumed in (8) and used to arrive at (9) breaks down at critical surface. We have used this method here, and (9) is reformulated as a variational problem corresponding to a Lagrangian $L$ so as to make $\delta L/\delta z = 0$ equivalent to (9). The Lagrangian $L$ corresponding to (9) is given by

$$L = r \left| \frac{\partial \varepsilon}{\partial r} \right|^2 - \iota k_0 r \left( \varepsilon \frac{\partial \varepsilon^*}{\partial \xi} - \varepsilon^* \frac{\partial \varepsilon}{\partial \xi} \right) - k_0^2 r \left[ \frac{n_1}{n_c}(1 - e^{-I}) - \frac{n_2}{n_c} e^{-I} \right] |\varepsilon|^2. \tag{15}$$

https://doi.org/10.1017/S0022377801001258 Published online by Cambridge University Press

Thus, the solution to the variational problem

$$\delta \iiint L \, dx \, dy \, dz = 0 \tag{16}$$

also solves the nonlinear Schrödinger equation (9). Using the trial wave function (Andreev et al. 1987)

$$\varepsilon(r,\xi) = \varepsilon_0(\xi) \exp\left(-\frac{r_\perp^2}{a^2(\xi)} - \frac{\iota k_0 r_\perp^2}{2a(\xi)} \frac{da}{d\xi}\right), \tag{17}$$

we can integrate over $r_\perp$ to find $\langle L \rangle$ as

$$\langle L \rangle = \langle L_0 \rangle + \langle L_1 \rangle, \tag{18}$$

where

$$\langle L_0 \rangle = \frac{|\varepsilon_0(\xi)|^2}{2} - i\frac{k_0 a^2(\xi)}{4}\left(\varepsilon_0 \frac{\partial \varepsilon_0^*}{\partial \xi} - \varepsilon_0^* \frac{\partial \varepsilon_0}{\partial \xi}\right) + \frac{k_0^2 a^3}{8} \frac{d^2}{d\xi^2} |\varepsilon_0(\xi)|^2 \tag{19a}$$

$$\begin{aligned} \langle L_1 \rangle = &-\frac{k_0^2 a^2}{4} \frac{n_1}{n_c} \left[\varepsilon_0^2 - E_p^2 \left(1 - \frac{n_1}{n_c}\right)^{1/2} (1 - e^{-I_0})\right] \\ &+ \frac{k_0^2 a^2}{8} \frac{E_p^2}{L_\perp^2} \left(1 - \frac{n_1}{n_c}\right)^{1/2} [E_1(I_0) + \ln I_0 + C] \end{aligned} \tag{19b}$$

where $E_1(I_0)$ is the exponential integral (Abramowitz and Stegun 1965), $C = 0.57721$ is Euler's constant, and

$$I_0 = \frac{(\varepsilon_0/E_p)^2}{N_\parallel(\xi)}. \tag{20}$$

It must be mentioned that in evaluating the integrals appeared in (16), we have used standard results (Abramowitz and Stegun 1965). Further, using the procedure of Anderson et al. (1979) and Anderson (1983) as well as Karlsson et al. (1992), it is possible to arrive at the following equations for the beam width $a$ and the longitudinal phase delay $\phi$ :

$$\begin{aligned} \frac{d^2 a}{d\xi^2} = &\frac{8}{k_0^2 a^3} + \frac{4n_1}{a n_c}\left[e^{-I_0} - \frac{1}{I_0}(1 - e^{-I_0})\right] \\ &- \frac{4a}{I_0 L_\perp^2}[E_1(I_0) + \ln\, I_0 + C - \tfrac{1}{2}(1 - e^{-I_0})] \end{aligned} \tag{21}$$

$$\begin{aligned} \frac{d\phi}{d\xi} = &\frac{3}{k_0 a^2} - k_0 \frac{n_1}{n_c}\left[\tfrac{1}{2} - \tfrac{3}{2}e^{-I_0} + \frac{1}{I_0}(1 - e^{-I_0})\right] \\ &- \frac{k_0 a^2}{L_\perp^2 I_0}[E_1(I_0) + \ln\, I_0 + C - \tfrac{3}{4} + \tfrac{3}{4}e^{-I_0}]. \end{aligned} \tag{22}$$

It is convenient to work in dimensionless variables. For this purpose, we introduce the following transformations:

$$z = -L_\parallel \zeta^2, \qquad N_\parallel = \zeta \qquad \text{for } 0 < \zeta < 1, \tag{23a,b}$$

$$\frac{n_1}{n_c} = 1 + \frac{z}{L_\parallel}, \qquad \xi = 2L_\parallel(1 - N_\parallel(z)) \tag{23c,d}$$

https://doi.org/10.1017/S0022377801001258 Published online by Cambridge University Press

and arrive at the following simplified equations for the beam width and phase:

$$\frac{d^2a}{d\zeta^2} = \frac{32L_\parallel^2}{k_0^2a^3} - \frac{16L_\parallel^2}{a}(1-\zeta^2)\left[\frac{1}{I_0}(1-e^{-I_0}) - e^{-I_0}\right]$$
$$-\frac{16aL_\parallel^2}{I_0L_\perp^2}[E_1(I_0) + \ln I_0 + C - \tfrac{1}{2}(1-e^{-I_0})] \tag{24}$$

and

$$\frac{d\phi}{d\zeta} = -\frac{6L_\parallel}{k_0a^2} + 2k_0L_\parallel(1-\zeta^2)\left[\tfrac{1}{2} - \tfrac{3}{2}e^{-I_0} + \frac{1}{I_0}(1-e^{-I_0})\right]$$
$$+\frac{2k_0a^2L_\parallel}{I_0L_\perp^2}[E_1(I_0) + \ln I_0 + C - \tfrac{3}{4} + \tfrac{3}{4}e^{-I_0}]. \tag{25}$$

To cast these two equations in more succinct form, the well-known terminology used in self-focusing phenomenon is considered. For this purpose, we introduce the length scale of nonlinear refraction $R_{nl} = E_p/\sqrt{2\varepsilon_0}$, the diffraction length $R_g = \frac{1}{2}k_0a_0^2$ and the dimensionless beam width $A = a/a_0$. Then (24) and (25) can be rewritten in the following forms:

$$\frac{d^2A}{d\zeta^2} = \frac{8L_\parallel^2}{R_g^2A^3} - \frac{16L_\parallel^2}{Aa_0^2T}(1-\zeta^2)[1-(1+T)e^{-T}]$$
$$-\frac{16AL_\parallel^2}{TL_\perp^2}[E_1(T) + \ln T + C - \tfrac{1}{2}(1-e^{-T})] \tag{26}$$

and

$$\frac{d\phi}{d\zeta} = -\frac{3L_\parallel}{R_gA^2} + \frac{4R_gL_\parallel}{a_0^2T}(1-\zeta^2)\left[T\left(\tfrac{1}{2} - \tfrac{3}{2}e^{-T}\right) + 1 - e^{-T}\right]$$
$$+\frac{4A^2R_gL_\parallel}{TL_\perp^2}[E_1(T) + \ln T + C - \tfrac{3}{4} + \tfrac{3}{4}e^{-T}], \tag{27}$$

where

$$T = \frac{1}{2R_{nl}^2\zeta}$$

## 3. Discussion

Equations (26) and (27) are not amenable to analytical solution. Equation (26), representing the evolution of the normalized beam width, is very important and contains significant physics (cf. equation 2.1 of Andreev et al. 1987). The right-hand side of (26) contains three terms, each emanating from different physical concept contained in (9). The first term on the right-hand side of (26), representing spatial dispersion, leads to diffractional divergence in the absence of nonlinear terms. The additional factor of $L_\parallel^2$ appearing in the numerator of this term results from the longitudinal inhomogeneity introduced in the direction of propagation. The second term in (26), arising on account of ponderomotive nonlinearity (the second term on the right-hand side of (9)), prevents the spread of flow by counteracting the diffractional divergence. Its peculiar form has its origin in the particular form of the

https://doi.org/10.1017/S0022377801001258 Published online by Cambridge University Press

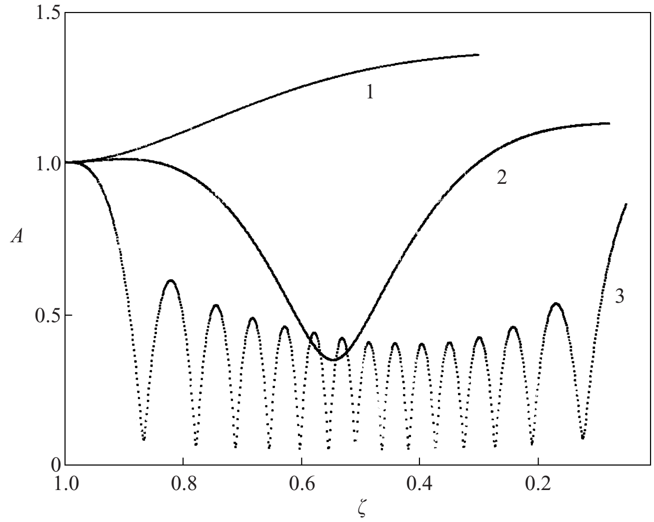


**Figure 1.** Variation of normalized beam width $A$ with dimensionless distance of propagation $\zeta$ for different $R_{nl}$ with $a_0 = 0.005\,\mathrm{cm}$, $R_g = 0.075\,\mathrm{cm}$, $L_{\|} = 0.075\,\mathrm{cm}$, and $L_{\perp} = 0.075\,\mathrm{cm}$. Curve 1 corresponds to $R_{nl} = 0.05$, curve 2 to $R_{nl} = 0.1$, and curve 3 to $R_{nl} = 0.5$.

trial function and is a consequence of the averaging process used in the variational approach. It is a major dominant term that although initially small, competes with the diffraction term to determine the overall evolution of beam width. A special feature of this term is that it contains inhomogeneity as well as $R_{nl}$. The last additional term comes from the relative inhomogeneity $(L_{\|}/L_{\perp})$ introduced into the problem as well as ponderomotive nonlinearity, and is a consequence of the last term on the right-hand side of (9). Likewise, it also evolves with $\zeta$, varying in the different regions of propagation, and also contributes to self-focusing. In the absence of the last term, the fate of the beam evolution is determined by the relative competition of the first two terms.

We have performed numerical computations of (26) and (27) using the Runge–Kutta method while maintaining a specific relationship between $R_g$, $R_{nl}$, $L_{\|}$, and $L_{\perp}$. In Fig. 1, the normalized beam width is plotted as a function of the dimensionless distance of propagation $\zeta$ for three different values of $R_{nl}$ and with other parameters chosen as follows:

$$a_0 = 0.005\,\mathrm{cm}, \qquad R_g = 0.075\,\mathrm{cm}, \qquad L_{\|} = 0.075\,\mathrm{cm}, \qquad L_{\perp} = 0.075\,\mathrm{cm},$$

There are several salient features observed in Fig. 1:

(a) A decrease in $R_{nl}$ results in overall weakening of the second and third terms, since it appears through $T$. This leads to overall dominance of diffraction phenomenon, resulting in self-defocusing of the beam, as is obvious from curve 1.

(b) The second term, which is vanishingly small in the initial stage (it is zero at $\zeta = 1$), evolves with $\zeta$, but in $(1 + T)e^{-T}$ the exponential factor overcomes the factor $1 + T$, resulting in weakening of this term for smaller $\zeta$.

(c) It is also observed that the nonlinearity plays a significant role only when the beam has undergone some propagation through the plasma. Thus diffraction is the dominant mechanism in the initial stage, as is obvious from curves 1 and 2.

https://doi.org/10.1017/S0022377801001258 Published online by Cambridge University Press

**Table 1.**

| | | | | | | | | | | | | | |
|---|---|---|---|---|---|---|---|---|---|---|---|---|---|
| $\zeta$ | 1.0 | 0.95 | 0.90 | 0.85 | 0.80 | 0.75 | 0.70 | 0.65 | 0.60 | 0.55 | 0.50 | 0.45 | 0.40 |
| $A$ | 1.00 | 1.00 | 1.00 | 1.00 | 1.00 | 1.00 | 1.00 | 1.00 | 1.00 | 1.00 | 0.999 | 0.999 | 0.999 |

Particularly in this stage, the last term counteracts the diffraction, preventing the steep rise in $A$, and defocusing is significantly slowed down when the second and third terms both contribute significantly. This becomes more apparent from curve 3.

(d) When the diffraction and nonlinear second terms are almost of the same order, the last term plays a significant role in self-focusing phenomenon. In such a case, when combined with the second term for the chosen set of parameters, it leads to oscillatory self-focusing. Each time a minimum in $A$ is achieved, the diffraction term becomes large, and after some increase in normalized beam width, focusing sets in again, with an overall effect of oscillatory self-focusing.

(e) As we approach the critical surface, the beam tends to defocus (curve 3) and focusing is slowed (curve 2). However, the theory is not valid in the neighbourhood of the critical surface ($\zeta = 0$). The theory breaks down completely in the neighbourhood of and at the critical surface. This is because the variation of $N_\|$ (expressed in $E$ through (7)) with $\zeta$ is assumed to be slow, and it is because of this that the derivatives of $N_\|$ have been neglected. On the other hand, $N_\|$ varies abruptly at or near the critical surface, and the present approach is not valid.

In the absence of the second term (longitudinal inhomogeneity), it is possible to find critical value of the power/intensity required for self-trapping of the beam. In such a case, the beam propagates in a self-generated waveguide mode without convergence or divergence. In the absence of the second term and with $\zeta = 1$ ($z = 0$), the condition for self-trapping results in the following equation:

$$\frac{L_\perp^2}{R_g^2} = 4R_{nl}^2[E_1(T_1) + \ln T_1 + C - \tfrac{1}{2}(1 - e^{-T_1})] = FN(R_{nl}), \tag{28}$$

where

$$T_1 = \frac{1}{2R_{nl}^2} = \frac{\varepsilon_0^2}{E_p^2}.$$

Since (28) is a trancendental equation, it must be solved numerically or graphically. We have used the latter approach here, where values of $L_\perp^2$ versus $R_g^2$ have been plotted. Then $FN(R_{nl})$ is plotted as a function of $R_{nl}$. It is observed that (28) is satisfied only for certain values of $R_{nl}$, $L_\perp^2$, and $R_g^2$. As is obvious from Fig. 2, there are two values of $R_{nl}$, corresponding to the intersection of the curves, for which (28) is satisfied. These, the only possible value of $R_{nl}$, determine the critical threshold power required for self-trapping of the beam. From these values, we can calculate $E_{\mathrm{cr1}}$ and $E_{\mathrm{cr2}}$. We have solved (26) (in the absence of the second term on the right-hand side) numerically, particularly for these values of $R_{nl}$. For example, when $R_{nl} = 1.0$, the other parameters are $L_\| = 0.075$, $R_g = 1.0$, and $L_\perp = 1.0$. Similarly, for the other value of $R_{nl}$, namely $R_{nl} = 1.50$, the other parameters are $L_\| = 0.075$, $R_g = 1.2247$, and $L_\perp = 1.2247$. The results of propagation for these two sets of values are shown in Table 1.

https://doi.org/10.1017/S0022377801001258 Published online by Cambridge University Press

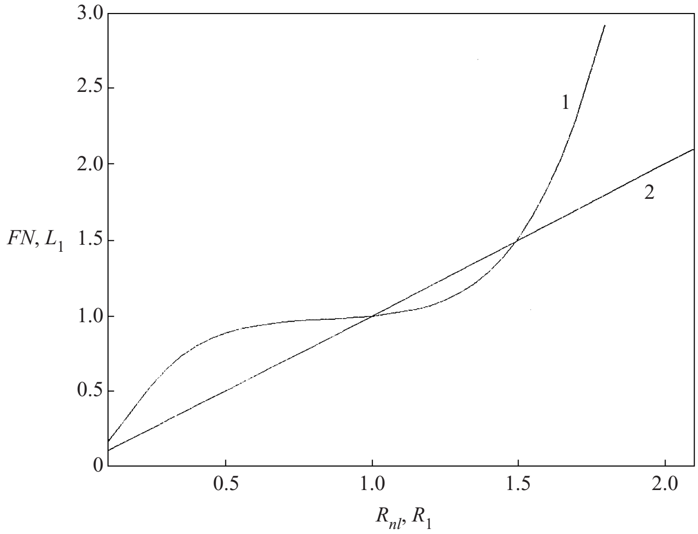


**Figure 2.** Variation of $FN(R_{nl})$ with $R_{nl}$ for various values of $L_1$ $(= L_\perp^2)$ and $R_1$ $(= R_g^2)$ with a fixed value of $L_\|$. Curve 1 is for $FN$ versus $R_{nl}$ and curve 2 for $L_1$ versus $R_1$.

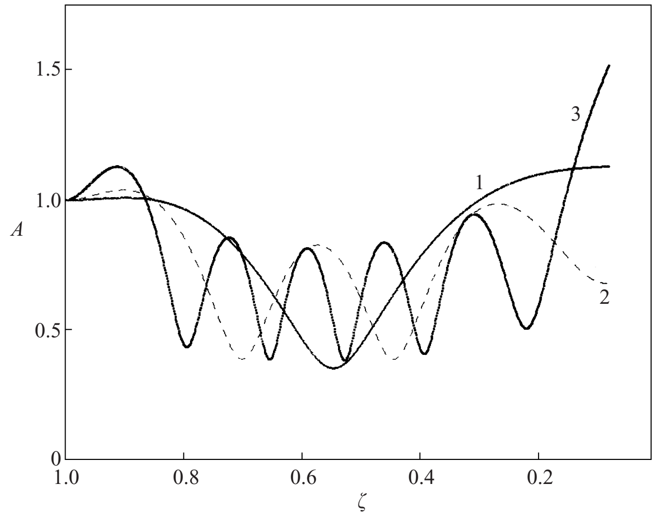


**Figure 3.** Variation of $A$ with $\zeta$ for different $L_r$ $(= L_\|/L_\perp)$ with $R_{nl} = 0.1$ cm, $R_g = 0.075$ cm, and $a_0 = 0.005$ cm. Curve 1 corresponds to $L_r = 1$, curve 2 to $L_r = 2$, and curve 3 to $L_r = 4$.

As is obvious from the table, it is observed that the normalized beam width $A$ $(= a/a_0)$ exhibits a self-trapping mode over a fairly long distance of propagation.

In order to observe the effect of inhomogeneity scale lengths, we have plotted the normalized beam width $A$ as a function of $\zeta$ for different values of $L_r$ $(= L_\|/L_\perp)$ corresponding to $R_{nl} = 0.1$, the other parameters being the same as mentioned earlier. The smaller the scale-length ratio of the inhomogeneity, the stronger is the self-focusing, as is apparent from Fig. 3. An initially defocusing curve exhibits focusing with distance of propagation. However, an increase in $L_r$ for the same value of $R_{nl}$ results in oscillatory self-focusing and defocusing. This results from variation

https://doi.org/10.1017/S0022377801001258 Published online by Cambridge University Press

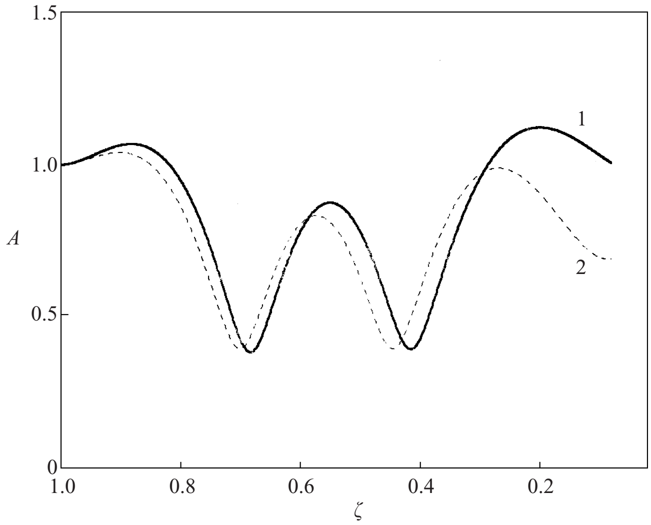


**Figure 4.** Variation of $A$ with $\zeta$ for longitudinal inhomogeneity and both scale lengths of inhomogeneity, with $L_r = 2.0$ and the other parameters the same as mentioned in the caption of Fig. 3. Curve 1 corresponds to longitudinal inhomogeneity and curve 2 to both scale lengths of inhomogeneities.

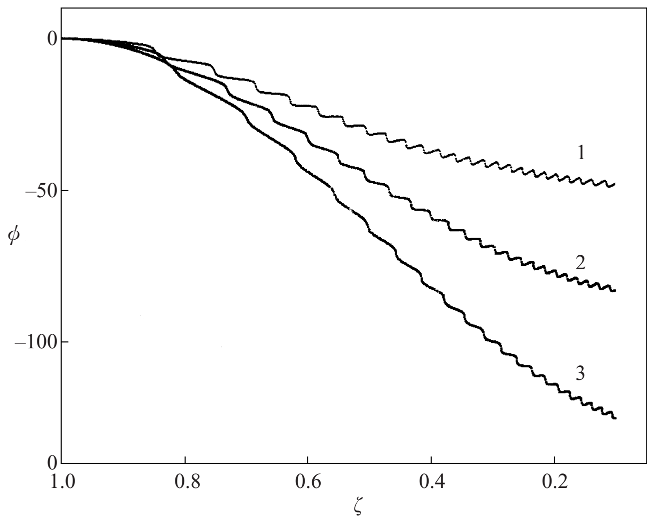


**Figure 5.** Plot of the longitudinal phase delay $\phi(\zeta)$ for different values of $R_{nl}$ and with the other parameters the same as mentioned in the caption of Fig. 1. Curve 1 corresponds to $R_{nl} = 1.0$, curve 2 corresponds to $R_{nl} = 1.2$, and curve 3 to $R_{nl} = 1.5$.

in the nonlinear focusing terms on the right-hand side of (26) with increasing $L_r$. Further, on increasing the value of $R_{nl}$, oscillatory self-focusing and strong defocusing with distance of propagation is observed. Nonetheless, the finer details of the critical balance between diffraction and nonlinear refraction cannot be determined in the neighbourhood of the critical surface, and the present approach is not suitable for such a study (Burge 1998).

https://doi.org/10.1017/S0022377801001258 Published online by Cambridge University Press

In order to identify the role of the addition of transverse inhomogeneity, we have plotted the beam width $A$ as a function of $\zeta$ for two cases:

(i) when $L_\perp$ is missing, i.e. only longitudinal inhomogeneity is present;

(ii) when both scale lengths of inhomogeneity are present.

In the absence of transverse inhomogeneity, as is obvious from curve 1 in Fig. 4, defocusing sets in the final stage of propagation. However, when both scale lengths are introduced, self-focusing is enhanced, as is observed in curve 2.

Lastly, Fig. 5 displays the longitudinal phase delay $\phi$ with $\zeta$ for various values of $R_{nl}$, with the other parameters remaining the same as mentioned earlier. For large $R_{nl}$, the phase is primarily due to the diffraction term, and the corresponding change in phase with distance of propagation is very small. However, with increasing $R_{nl}$, the nonlinearity contributes significantly, and the phase evolves as a monotonically decreasing function with propagation as well as preserving negative values throughout the transit. This compares well with the results obtained by Karlsson et al. (1992) for the case of nonlinear optical fibres.

*Acknowledgements*

This research work was supported by the Department of Science and Technology and the University Grants Commission of India. One of the authors (T.S.G) is thankful of Professor M. S. Sodha (ITM, Gurgaon), Professor R. P. Sharma (IIT, New Delhi) and Dr Arvind (GNDU, Amritsar) for valuable discussions.

## References

Abramowitz, M. and Stegun, I. A. 1965 *Handbook of Mathematical Functions* (ed. M. Abramowitz and I. A. Stegun). New York. Dover, p. 228.

Akhmanov, S. A., Sukhorov, A. P. and Khokhlov, R. V. 1968 *Soviet Phys. Usp.* **10**, 609.

Amin, M. R., Capjack, C. E., Frycz, P., Rozmus, W. and Tichonchuk, V. T. 1993 *Phys. Fluids* **5**, 3748.

Anderson, D. 1983 *Phys. Rev.* **A27**, 3135.

Anderson, D., Bonnedal, M. and Lisak, M. 1979 *Phys. Fluids* **22**, 1838.

Andreev, A. A. 1983 *Soviet Tech. Phys. Lett.* **9**, 438.

Andreev, A. A., Erokhin, N. S., Sutyagin, A. N. and Fadeev, A. P. 1987 *Soviet J. Plasma Phys.* **13**, 608.

Askar'yan, G. A. 1962 *J. Exp. Theor. Phys.* **42**, 1567.

Berge, L. 1997 *Phys. Plasmas* **4**, 1227.

Berge, L. 1998 *Phys. Rep.* **303**, 259.

Berger, R. L., Lam, B. F., Kaiser, T. B., Willium, E. A., Langdon, A. B. and Cohen, B. I. 1993 *Phys. Fluids* **5**, 2243.

Chio, R. Y., Garmire, E. and Townes, C. H. 1964 *Phys. Rev. Lett.* **13**, 479.

Cohen, B. I., Lasinski, B. F., Langdon, A. B. and Cummings, J. C. 1991 *Phys. Fluids* **3**, 766.

Karlsson, M., Anderson, D. and Desiak, M. 1992 *Opt. Lett.* **17**, 22.

Kaw, P., Schmidt, G. and Wilcox, T. 1973 *Phys. Fluids* **16**, 1522.

Kelly, P. L. 1965 *Phys. Rev. Lett.* **15**, 1005.

Kruer, W. L. 1988 *The Physics of Laser Plasma Interactions*. Redwood city, CA: Addison-Wesley.

Lam, J. F. and Lippman, B. 1977 *Phys. Fluids* **20**, 1176.

Malkin, V. M. 1993 *Physica* **D64**, 251.

Max, C. E. 1976 *Phys. Fluids* **19**, 74.

https://doi.org/10.1017/S0022377801001258 Published online by Cambridge University Press

Paisner, J. A., Boyes, J. D., Kumpan, S. A., Lowdermilk, W. H. and Sorem, M. S. 1994 *Laser Focus World* **30**, 75.

Perkins, F. W. and Valeo, E. J. 1974 *Phys. Rev. Lett.* **32**, 1234.

Schmidt, A. J. 1988 *Phys. Fluids* **31**, 3079.

Sodha, M. S., Ghatak, A. K. and Tripathi, V. K. 1976 *Prog. Opt.* **13**, 169.

Sodha, M. S., Singh, T., Singh, D. P. and Sharma, R. P. 1981 *Phys. Fluids* **24**, 914.

Subbarao, D., Uma, R. and Singh, H. 1998 *Phys. Plasmas* **5**, 3440.

Sughiara, R. and Nishimura, K. 1995 *J Phys. Soc. Jpn* **64**, 4156.

Sulem, C. and Sulem, P. L. 1999 *The nonlinear Schrödinger Equation*. Berlin: Springer–Verlag.

Talanov, V. I. 1965 *Soviet Phys. JETP Lett.* **2**, 138.

Tikhonchuk, V. T. Hullar, S. and Mounaix, P. H. 1997 *Phys. Plasmas* **4**, 4369.

Vlasov, S. N., Petrischev, V. A. and Talanov, V. I. 1971 *Soviet Rad. Phys. Quantum Electron.* **14**, 1962.

Wagner, W. G., Haus, H. A. and Marburger, J. H. 1968 *Phys. Rev.* **175**, 256.

Zakharov, V. I. 1972 *Soviet Phys. JETP* **35**, 908.

https://doi.org/10.1017/S0022377801001258 Published online by Cambridge University Press